From Complexity to Consistency: Reframing Fault Response Requirements for Inverter-Based Resources

Bogdan Kasztenny and Normann Fischer
Schweitzer Engineering Laboratories, Inc.

Ali Hooshyar
University of Toronto

Presented at the
53rd Annual Western Protective Relay Conference
Spokane, Washington
October 27–29, 2026

Originally released February 2026

From Complexity to Consistency: Reframing Fault Response Requirements for Inverter-Based Resources

Bogdan Kasztenny and Normann Fischer, *Schweitzer Engineering Laboratories, Inc.*
Ali Hooshyar, *University of Toronto*

***Abstract*—This paper proposes a new framework for inverter-based resource (IBR) fault response requirements in high-voltage networks. Standards, such as IEEE Std 2800, rely on phasor-based specifications and permit generous IBR response times, leading to inconsistent behavior during the critical first power cycles of a fault. We propose a simple time-domain IBR specification that prioritizes speed, current-voltage consistency, and incremental currents, including the negative-sequence component, rather than total currents. The proposed method "freezes" the positive-sequence controller and phase-locked loop at fault inception and emulates a virtual shunt reactor to maintain network homogeneity and expected signal relationships during fault conditions. This approach eliminates the need for detailed IBR modeling when setting instantaneous protection, supports traditional protection principles, and enables advanced protection concepts, offering a practical path forward without added cost or complexity.**

I. Introduction

The response of inverter-based resources (IBRs) during fault conditions remains a major research topic and a focus of ongoing standardization efforts by national, regional, and international organizations. Despite these efforts, progress has been limited, and protection engineers remain concerned about the consistency of IBR fault response. Today, modeling and simulation are widely used to design protection systems for networks near IBRs. Changes in IBR control algorithms (e.g., firmware updates) or configuration (e.g., user-controllable setpoints) can jeopardize protection systems and require re-engineering. Although this model-based approach was initially unavoidable, it is not sustainable in the long term.

Historically, the protection community has viewed its role as protecting the apparatus rather than influencing its behavior. This view initially led to the belief among many protection practitioners that IBR fault response standardization was unnecessary, and only gradually was the need for standardization recognized. Developing standards took additional time, followed by IBR manufacturers implementing the early versions of fault response standards. IBR manufacturers operate under significant cost pressures, which further constrain what can be achieved through consensus in standardization efforts. The standards remain unharmonized across regions, and IBR manufacturers routinely deliver systems customized for regional or end-user requirements. All these factors led to a situation where a significant IBR installed base exists while the fault response standardization is weak or nonexistent.

One reason for the lack of success in standardizing IBR fault response is a limited understanding of both protection challenges and potential solutions. No established practices were available to guide standardization, so the standardization bodies often invented solutions as a part of committee work. Standards in use are experimental at the cost of users and manufacturers.

Synchronous generators (SGs) respond to faults in a manner dictated by physical laws and largely independent of design and materials. For more than a century, protective relays have evolved to leverage these persistent fault signal characteristics. For example, the angle between the zero- and negative-sequence currents is a reliable indicator of fault type and has become a de facto standard for faulted-loop selection logic in distance protection elements.

IBR fault response is also constrained by physical limits, such as the semiconductor device thermal rating and the dc bus capacitor voltage rating. However, within these boundaries, the response can vary significantly and depends heavily on the IBR control algorithms.

Although IBR fault response cannot match SG response in current magnitude or in phase relative to voltage, standardization efforts have nonetheless attempted to guide IBRs toward two SG-like attributes. First, the standards sought to increase the reactive content of the positive-sequence current, thereby shifting its angle to resemble that of an SG, originally with system stability objectives rather than protection considerations. Second, they aimed to adjust the relative magnitudes of the positive- and negative-sequence current components to more closely match those of an SG. While well intentioned, the methods adopted to achieve these two goals have proven inadequate for several reasons:

- Inverter semiconductor devices restrict phase currents to approximately 1.2 to 1.5 pu, with a possible future increase to about 2 pu. Cost pressures will continue to favor sizing semiconductor devices for load rather than fault conditions, making these limits persistent even when higher-rated semiconductor devices become available.
- Fault response timing requirements, such as low-voltage ride-through (LVRT) or negative-sequence current injection, remain generous, typically several power cycles, but protection must often operate much faster.

- Although overall response time allowances are generous, IBR control actions often begin within milliseconds, creating significant signal anomalies during the first few cycles of a fault, precisely when protection action is most critical.
- Standards specify and manufacturers implement fault response by using complex mechanisms – dead bands, signal limiters, and inherent delays caused by phasor-based processing. Many aspects of IBR design, especially controls, remain proprietary. As a result, users cannot characterize IBR fault response without modeling each installation individually. Can we call it a standard if installation-specific modeling is still required?
- IBR fault response does not align with protection system operating time frames. For example, ultra-high-speed relays [1] paired with fast breakers can clear faults in as little as 1.5 cycles (25 ms at 60 Hz) [2], which is faster than the time allowance for a negative-sequence response to stabilize. For example, the step response time and the settling time in IEEE 2800 are 2.5 and 4 cycles, respectively.

Because of these factors, the industry faces the worst of both worlds: IBRs aggressively modulate relay input signals during faults, creating challenges for protective relays, and IBRs also overreact by not recognizing that faults in high-voltage systems are short-lived, adding unnecessary disturbances to the system.

This paper aims to reset the approach to IBR fault response standardization with the following objectives:

1. Simplify the IBR fault response so engineers can configure and validate protection systems without detailed modeling. A successful standard eliminates the need for modeling beyond a conventional short-circuit study.
2. Ensure implementation without added cost or complexity.
3. Limit the scope of standardized fault response characteristics while meeting expectations rooted in SG behavior.
4. Establish clear boundaries between the roles of protection systems and IBRs to enable successful integration without custom engineering.
5. Make the IBR fault response persistent and unlikely to change over time, preventing unnecessary IBR innovation while not hindering innovation in other areas.

In essence, we advocate standardizing less but doing it better and with simplicity. If the fault response is truly standardized, one should be able to envision relay voltage and current signals during fault conditions without knowing the IBR make, model, firmware revision, or setpoints.

II. Fault Signal Characteristics Subject to IBR Standardization

Given the limitations of IBRs, it is practical and sufficient to ensure the following fault signal relationships.

A. Initial Fault Response

Traditional relays protecting high-voltage systems operate on approximately 1 cycle of fault data. Ideally, an IBR should respond to a fault within a few milliseconds and maintain a stable fault response for the first few cycles. A successful standard must emphasize an instantaneous response within a fraction of a cycle rather than allowing generous margins for settling the mandated fault signal characteristics.

Beyond the first few cycles, optimizing the IBR response for protective relays during slowly cleared faults offers diminishing returns. After a normal fault clearing time of a few cycles, an IBR may pursue other control objectives. Modern relays should treat the subsequent IBR fault response for slowly cleared faults as a contingency if they have already received a few cycles of a favorable fault response.

Our approach shifts the focus from generous time allowances to an instantaneous but time-limited IBR fault response. We recommend at least 2 cycles of IBR fault response tailored for protective relays. The longer, the better. As we show in this paper, providing a longer response is not difficult. One may consider a time interval equal to the normal fault clearing time or the fault clearing time that includes a breaker failure contingency.

An instantaneous IBR response requires time-domain implementation rather than phasor-based implementation. Framing the IBR fault response in phasor terms is, therefore, a major problem in present-day practice.

B. Voltage vs. Current Response

An IBR does not – and likely will not – behave like an ideal voltage source behind a fixed and relatively small impedance. Therefore, during the first few cycles, treating the IBR as a current source is beneficial: the system dictates voltages, and the IBR produces currents coherent with those voltages, thus preserving the voltage-current relationships used by protective relays.

In essence, during the first few cycles of the fault, we do not rely on the IBR to maintain voltage or provide reactive power support. We only require the source to produce currents that remain coherent with the voltages that the network forces on the IBR.

C. Currents vs. Incremental Currents

IBR fault currents cannot emulate the level of SG fault currents. However, incremental IBR fault currents – defined as the change between the present instantaneous values and the several-cycles-old values – can and should emulate incremental fault currents observed in the SG-dominated networks. This approach allows protective relays to maintain expected behavior without requiring the IBRs to produce SG-like total currents.

To drive such incremental currents, we select a fictitious source impedance – a shunt impedance that mathematically connects the incremental voltages and currents – so that incremental currents during close-in faults remain within the 0.2 to 0.5 pu headroom that the IBR can provide during fault conditions. This approach ensures that the IBR contributes meaningful fault currents without exceeding its physical limits.

In electric power networks, incremental voltages and currents follow the first-order differential equation that describes the RL nature of the circuit. For forward faults, this relationship reflects the circuit behind the relay; for reverse faults, it reflects the circuit in front of the relay. This concept has been formalized through the replica current principle and has been used in directional protection for nearly a century [1].

We propose that a successful IBR fault response standard mandates magnitude-limited incremental phase currents. Doing so inherently guarantees proper incremental positive-sequence current as well as negative-sequence current. In essence, although the IBR cannot provide an SG-like total fault current level, it can deliver SG-like incremental fault currents. In Section VII, we demonstrate that an IBR can produce incremental currents with fidelity and without time lag so that these incremental currents retain the expected relationships with the voltages.

Many modern protective relays already operate based on incremental voltages and currents, a technology that has existed for decades. Implementing incremental quantity-based logic in protective relays is straightforward and free from intellectual property restrictions.

D. Negative-Sequence Response

Negative-sequence voltage and current are types of incremental quantities because under normal load conditions, they remain at near zero. Therefore, when incremental phase currents are provided in a manner coherent with incremental voltages, the expected relationship between the negative-sequence voltage and the negative-sequence current is inherently satisfied.

In our approach, the negative-sequence voltage-current relationship takes the form of a fixed impedance. We must select this impedance so that its magnitude limits the phase current to within the available IBR headroom during fault conditions. This requirement ensures that the IBR preserves the expected fault current pattern without exceeding its physical limits.

In addition, we must select a highly inductive impedance that ties together voltages and currents, including phase incremental, negative-sequence, and incremental positive-sequence quantities. This highly inductive impedance maintains the homogeneity of the network. Preserving network homogeneity is essential because it ensures that the voltage-current relationships used by protective relays remain consistent throughout the system, regardless of whether the source is an SG, an IBR, or a combination of both.

E. Source Inertia and Memory Polarization in Relays

Protection element designs, especially those for directional and mho distance elements, assume high source inertia and use the pre-fault voltage angle as a proxy for the fault voltage angle, particularly when the voltage is too small to be reliably measured, such as during close-in bolted three-phase faults. Therefore, a successful IBR fault response standard should maintain the pre-fault position (angle) and velocity (frequency) of the phase-locked loop (PLL) during the first few cycles of the fault.

We can meet this requirement by "freezing" the PLL, allowing it to "free wheel" when a fault is detected, or by switching to longer time constants in the PLL after it has locked and is tracking the voltage. The to-date IBR field experience teaches us that rapid tracking of the system voltage angle during faults is counterproductive.

III. Implementation

A. Overview

We implement the proposed approach by using a few simple modules, as illustrated in Fig. 1. For clarity, we start with phase currents instead of the dq reference frame commonly used by the IBR designers.

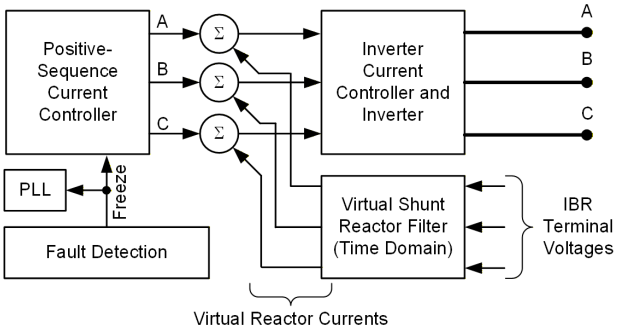


Fig. 1. Simplified block diagram of the IBR fault controller.

1) Positive-Sequence Current Controller

The positive-sequence current controller regulates only the positive-sequence current. Designed for current and power control during normal (fault-free) operation, this controller does not modulate the negative-sequence current. This controller should maintain the pre-fault PLL angle and positive-current references during the initial stage of a fault. We recommend a minimum delay of 2 cycles, although longer intervals are achievable as well. Effectively, an IBR should provide the fault response and refrain from executing other control actions for the duration of the normal fault clearing time (3 to 4 cycles) or the fault clearing time under a breaker failure contingency (9 to 11 cycles).

2) Fault-Detection Module

This module freezes the reference points of the positive-sequence current controller and the PLL. This module is not required if both the positive-sequence controller and the PLL use long time constants and do not react to a fault within the first few cycles. If implemented, the module can be a simple instantaneous undervoltage element that uses short-window phasors. If the fault-detection module triggers inadvertently under load conditions, such as during switching operations in the system, the proposed logic will not alter IBR currents because these currents would remain constant even if not frozen. As a result, the sensitive fault-detection module does not cause any unintended consequences.

3) Virtual Shunt Reactor Module

This module calculates phase current samples from phase-to-phase voltage samples by modeling a virtual shunt reactor at the IBR terminals. The reactor currents are referenced with

polarity toward the IBR terminals rather than the neutral point, and therefore, they are added and not subtracted in the control system in Fig. 1. From the signal-processing perspective, this module is a simple infinite impulse response (IIR) filter. Section IV provides implementation details. We select the reactor impedance to limit incremental currents so that the IBR phase currents remain within the available IBR headroom during close-in faults. To maintain network homogeneity, we select the reactor X/R ratio to provide an impedance angle congruent with the positive-sequence impedance of the system.

4) Inverter Current Controller

We sum the phase currents from the frozen positive-sequence controller and the currents from the virtual reactor and send the combined signals to the inverter current controller that performs current modulation and synthesis. These composite phase current signals may include decaying dc offsets and higher-frequency components. However, the high switching frequencies of modern inverters allow them to reproduce these signals with sufficient fidelity and minimal time lag.

During load conditions, the virtual shunt reactor draws a virtual positive-sequence current. The positive-sequence controller, being a closed-loop controller, accounts for the virtual shunt reactor when regulating power. Because the virtual current is reactive, the positive-sequence controller will effectively cancel it in the summing block shown in Fig. 1 by modulating the phase angle of the reference current.

During fault conditions, the depressed voltage reduces the IBR output power. In our approach, the closed-loop controller does not attempt to maintain the reference power, either because its time constant is sufficiently long or because the controller is intentionally prevented from enforcing the power reference during the initial few cycles of a fault.

Fig. 1 shows phase currents (ABC) to illustrate the concept from the viewpoint of first principles. Traditionally, IBR controls operate in the dq reference frame. Nonetheless, our concept remains applicable. The positive-sequence controller produces the dq-frame current, and the inverter current controller receives the dq-frame current. To implement our proposed method, we must transform the virtual reactor phase currents into the dq frame by using the PLL associated with the IBR (see Fig. 2).

Of course, the IBR is ungrounded just like an SG, and all three IBR phase currents have always only two degrees of freedom (d and q because $i_0 = 0$).

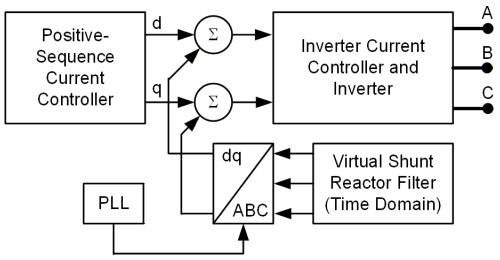


Fig. 2. Implementing the method in the dq reference frame.

B. Effective System Response

The proposed system is best understood by examining its effective response. A fault affects voltages at the IBR terminals, and these voltage changes cause corresponding changes in the virtual shunt reactor currents. The inverter then reproduces these changes, causing proportional changes in the IBR terminal currents. Consequently, the incremental terminal currents are coherent with the IBR terminal voltages as if a physical shunt reactor were present. Because the positive-sequence controller does not modulate the positive-sequence current but instead keeps it at the pre-fault value, the IBR current changes represent true incremental currents related to the incremental voltages.

The phase, positive-sequence, and negative-sequence impedances of the virtual reactor are identical. Therefore, the incremental loop currents (ΔI_{LOOP}), incremental positive-sequence current (ΔI_1), and negative-sequence current (I_2) all follow the same impedance, Z:

$$\Delta \mathrm{I}_{\mathrm{LOOP}} = -\frac{\Delta \mathrm{V}_{\mathrm{LOOP}}}{\mathrm{Z}}$$
$$\Delta \mathrm{I}_1 = -\frac{\Delta \mathrm{V}_1}{\mathrm{Z}},\ \Delta \mathrm{Z}_1 = -\frac{\Delta \mathrm{V}_1}{\Delta \mathrm{I}_1} \quad (1)$$
$$\mathrm{I}_2 = -\frac{\mathrm{V}_2}{\mathrm{Z}},\ \mathrm{Z}_2 = -\frac{\mathrm{V}_2}{\mathrm{I}_2}$$

The term loop relates to the traditional concept of distance and directional protection loops AG, BG, CG, AB, BC, and CA [1]. Equation (1) uses phasors for incremental loop quantities (frequency domain), but the same relationship applies to instantaneous incremental loop replica current and incremental loop voltage (time domain), as follows [1]:

$$\Delta \mathrm{i}_{\mathrm{Z}} = -\frac{\Delta \mathrm{v}}{|\mathrm{Z}|} \quad (2)$$

We will illustrate (1) and (2) in Section VII.

The incremental currents are proportional to the incremental voltages. If the fault-detection module triggers inadvertently because of a transient during load conditions, the incremental voltages will be small and short-lived, resulting in incremental IBR currents that are likewise small and transient. These incremental voltages and currents would be in a relationship that is consistent with the direction of the transient. This correct directional response is both desirable and consistent with traditional systems that include SGs.

It is worth clarifying that the interconnecting transformer remains transparent in the proposed approach, similar to a synchronous generator step-up (GSU) transformer or any other power transformer in the network.

IV. Virtual Shunt Reactor Filter

A. Derivation

We obtain the desired incremental currents by modeling a symmetrical shunt reactor, as shown in Fig. 3. The reactor is ungrounded to prevent zero-sequence current flow. We select the phase impedance (R and L values) to keep the incremental current within the IBR semiconductor device limits and to

preserve the desired system homogeneity angle (e.g., 86 degrees).

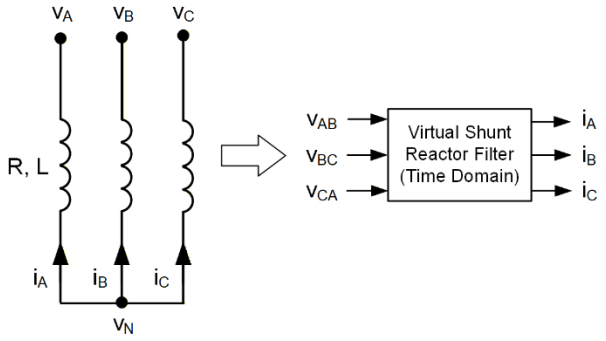


Fig. 3. Virtual shunt reactor principle and filter.

The following differential equations describe the circuit in Fig. 3 in the time domain:

$$\begin{aligned} i_A + i_B + i_C &= 0 \\ R \cdot i_A + L \cdot \frac{di_A}{dt} &= -(v_A - v_N) \\ R \cdot i_B + L \cdot \frac{di_B}{dt} &= -(v_B - v_N) \\ R \cdot i_C + L \cdot \frac{di_C}{dt} &= -(v_C - v_N) \end{aligned} \tag{3}$$

The minus signs in front of the voltages in (3) account for the assumed current direction. We discretize (3) at the sampling frequency f_S, by using the two-point trapezoidal formula as follows (k is the sample index):

$$\begin{aligned} \frac{dx}{dt} &\rightarrow f_S \cdot \left(x_{(k)} - x_{(k-1)}\right) \\ x &\rightarrow \frac{1}{2}\left(x_{(k)} + x_{(k-1)}\right) \end{aligned} \tag{4}$$

We substitute (4) into (3), solve for the currents, and obtain:

$$\begin{aligned} i_{A(k)} &= G_I \cdot i_{A(k-1)} - \\ G_V &\cdot \left(v_{AB(k)} - v_{CA(k)} + v_{AB(k-1)} - v_{CA(k-1)}\right) \end{aligned} \tag{5}$$

where the filter gains are:

$$\begin{aligned} G_V &= \frac{1}{6 \cdot (2 \cdot L \cdot f_S + R)} \\ G_I &= \frac{2 \cdot L \cdot f_S - R}{2 \cdot L \cdot f_S + R} \end{aligned} \tag{6}$$

We obtain the B- and C-phase currents by rotating the indices in (5).

Equations (5) and (6) represent a simple IIR filter that enables the IBR controller to compute the present samples (k) of the reactor phase currents based on the present (k) and previous (k–1) instantaneous voltage samples.

Key observations:

- The filter uses phase-to-phase voltages, as expected for a high-impedance IBR grounding (phase-to-ground voltages are unspecified for ungrounded systems).
- The filter is recursive but remains numerically stable because the reactor model shown in Fig. 3 includes resistance ($G_I < 1$ in (6) as long as $R > 0$).
- The calculated currents obey the physical laws of a reactor. Specifically, they may include a decaying dc offset and off-nominal frequency components that are coherent with the off-nominal components in the IBR voltages.

B. Optional Low-Pass Prefiltering

Voltages at the IBR terminals may contain high-frequency components caused by faults and converter switching. The phase-to-phase voltages used in (5) are typically less distorted than the phase-to-ground voltages. Furthermore, the filter (5) integrates the current, and the signal integral attenuates high-frequency components. Nevertheless, applying a low-pass filter to the voltages before using them in (5) can be beneficial.

We recommend limiting the voltage bandwidth in (5) to approximately 500 Hz. This level of filtering introduces minimal group delay while supporting practical phasor-based and time-domain protection elements that operate at or near the system nominal frequency, respectively.

If implemented, the low-pass filter introduces a group delay at the system frequency. We can compensate for this delay by slightly reducing the angle of the virtual reactor impedance used to compute the filter gains in (6). See the next subsection for details.

Of course, an analog anti-aliasing filter is already present for a given sampling frequency f_S. Therefore, the phase compensation, if needed, should account for both filters applied to the voltages: the anti-aliasing filter and the explicit low-pass filter.

C. Group Delay and Time Lag Compensation

The proposed method for generating incremental currents at the IBR terminals is subject to the following short time delays:

- Analog anti-aliasing filters introduce a group delay to the voltage signals.
- Optional digital low-pass filters add an additional group delay to the voltage signals.
- The inverter response may transiently lag the reference current by a short interval, typically on the order of 1 ms.

All these delays cause the IBR terminal current to lag the ideal reactor current by a total time delay, ΔT. We compensate for this lag by reducing the reactor impedance angle used to calculate the R and L parameters in (6).

If Θ is the original design impedance angle (in degrees), and ΔT is the total time lag (in milliseconds) to be compensated at the nominal system frequency f_N (in Hz), then we calculate the compensated impedance angle as follows:

$$\Theta_{COMP} = \Theta - \Delta T \cdot f_N \cdot \frac{360}{1{,}000} \tag{7}$$

This adjustment reduces the impedance angle and keeps it below 90 degrees, thereby preserving the filter numerical stability (5). For example, at 60 Hz, we can compensate for a 1.0 ms delay by reducing the angle by approximately 21 degrees.

It may seem counterintuitive that making the impedance less inductive advances the current. However, lowering the

impedance angle advances the current because the current polarity is assumed to be toward the IBR terminals rather than the neutral point.

V. Alternative Derivation

To better illustrate the concept, we derive the proposed method from the sequence networks of an SG. For the first few cycles of a fault, we can represent an SG by a voltage source behind a generator transient impedance (X'_d) in the positive-sequence network and by a negative-sequence impedance in the negative-sequence network (Fig. 4a). By applying the Thevenin-Norton source equivalence (the principle of voltage-current source equivalency), we can modify the SG equivalent network and represent the SG by using a current source (Fig. 4b).

Recognizing that a practical IBR cannot supply high fault currents, we intentionally increase the two impedances in Fig. 4b and use:

$$|Z| \gg X'_d \text{ and } |Z| \gg |Z_2| \quad (8)$$

We select the value of Z to limit current changes during close-in faults to acceptable levels, as we explained earlier. The equivalent networks of the SG shown in Fig. 4a and the IBR implementing the proposed method shown in Fig. 4c are identical in kind, differing only in degree. The SG and IBR equivalent networks show notable symmetry and strong conceptual alignment.

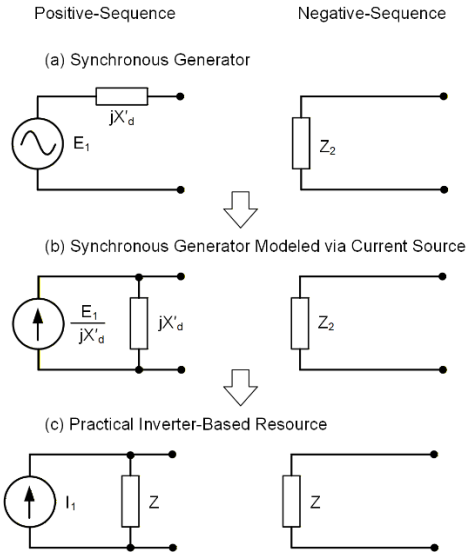


Fig. 4. Deriving the IBR equivalent network from an SG equivalent network.

Both the SG (Fig. 4a) and the IBR (Fig. 4c) equivalent networks include an ideal, perfectly balanced source with large inertia. In the SG equivalent network, the voltage source enables substantial fault current contribution, and its static behavior stems from the machine mechanical inertia. In contrast, the IBR equivalent network uses a current source, which aligns better with inverter-based technology. Its static behavior results either from an intentional freeze of the positive-sequence current controller and the PLL or from using deliberately long time constants in these two control subsystems. The intentionally high impedance limits the current changes at the IBR terminals during fault conditions.

Both equivalent networks also include a negative-sequence impedance. In the IBR equivalent network, this impedance is significantly larger than in the SG equivalent network to restrict the fault current to acceptable levels. The IBR negative-sequence impedance is virtual. Additionally, the IBR positive-sequence network includes a shunt impedance to make the current source implementation practical and to provide a path for the incremental current to follow the IBR voltages. This positive-sequence impedance is also virtual, and it does not affect the reactive power exchange with the connected power system.

Because the proposed method uses a simple virtual reactor to implement these impedances, the positive- and negative-sequence impedances are identical and equal to the phase impedance of the virtual reactor.

When we represent IBRs that comply with the proposed method, we can perform short-circuit calculations for the first few cycles of a fault by using the equivalent network shown in Fig. 4c.

VI. Summary of Protection Signal Characteristics

Our approach maintains the following signal relationships without compromise, ensuring that traditional protection principles perform correctly:

- The negative-sequence current remains coherent with the negative-sequence voltage, supporting negative-sequence directional elements used in line directional comparison schemes and optionally in distance protection elements.
- By being coherent with the negative-sequence voltage, the negative-sequence current is inherently coherent with the zero-sequence current originating at system grounding points. This coherence ensures correct operation of traditional fault-type identification logic in distance elements and in single-pole tripping applications.
- By following network homogeneity and being coherent with the zero-sequence current, the negative-sequence current can be used to polarize reactance comparators in quadrilateral distance elements and impedance-based fault locators. This capability is especially important for phase-to-phase and symmetrical three-phase faults, which do not benefit from the zero-sequence system response of the interconnecting transformer.
- The incremental positive-sequence current is coherent with the incremental positive-sequence voltage, enabling the use of incremental-quantity directional protection elements for symmetrical three-phase faults.
- The incremental phase (loop) currents remain coherent with the incremental phase (loop) voltages, allowing directional protection for all fault types, particularly phase-to-phase and symmetrical three-phase faults.
- The zero-sequence voltage and the zero-sequence current remain IBR-independent and coherent because of the interconnecting transformer. They support

directional protection elements and polarization of ground distance elements during ground faults.
- A frozen PLL ensures that memory polarization works effectively.
- The concept of apparent impedance remains valid, at least for bolted and low-resistance faults, regardless of the loop current characteristics [3]. Consequently, distance protection elements operate correctly if the faulted-loop selection logic, the voltage polarization for mho distance elements, and the current polarization for quadrilateral distance elements function correctly, as described above.

Our approach assumes that the positive-sequence current remains frozen during the first few cycles of the fault. Maintaining this fixed state is essential in order to prevent unintended modulation of the phase incremental currents.

In essence, the IBR fault currents produced by our method resemble currents during a high-resistance or remote fault: the fault currents are dominated by the pre-fault positive-sequence load component, with only small incremental components caused by the fault. Protective relays already handle high-resistance faults effectively, so expecting proper performance with IBRs that follow our approach is not a significant leap.

It is useful to summarize the protection principles that remain challenged even when using the proposed method. We identify two:

- Phase overcurrent protection (50/51, 67) remains challenged because the phase current is limited and not sufficiently inductive with respect to the voltage. However, this protection principle is not widely applied in high-voltage networks.
- Remote backup protection that uses distance elements (21T) also remains challenged because the low fault current magnifies the remote infeed effect. We can address this issue by applying the solutions presented in [3] or by shifting from remote backup protection to local backup protection, including breaker failure protection, direct transfer tripping, and redundancy.

VII. Illustration Examples

This section presents examples of relay operation in a system with an IBR that follows our fault response method. The study uses a detailed PSCAD EMTDC model of an inverter integrated in a modified version of the CIGRE North American high-voltage benchmark system [4]; see Fig. 5.

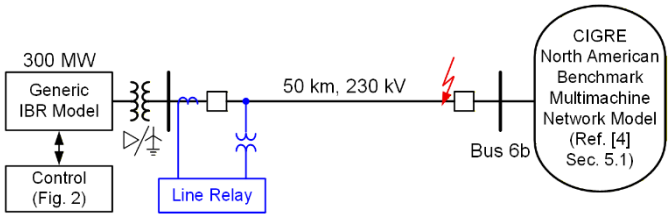


Fig. 5. Simplified system model.

A. Model Description

In the original CIGRE benchmark system, an SG at Bus 6b supplies 300 MW and 170 MVAR of power. In our model, we replaced this generator with a 300 MW IBR. To provide adequate reactive support, we increased the shunt capacitor bank at Bus 6b from 180 MVAR to 360 MVAR. We also added a 50 km, 230 kV transmission line to connect the IBR to the system at Bus 6b. The impedance of this line is identical, on a per-unit length basis, to the other 230 kV lines in the CIGRE benchmark system.

The IBR plant in Fig. 5 consists of 300 one-megawatt inverters. We modeled one inverter in detail and represented the remaining inverters by using an aggregator model [5]. The currents from all inverters flow through a 34.5 kV collector system represented by a π-circuit with a series resistance of 0.016 pu, a series reactance of 0.059 pu, and a shunt capacitive reactance of 31.25 pu, all on a 300 MVA, 34.5 kV base. The IBR unit transformers have a delta-wye-grounded connection and have a leakage reactance of 0.05 pu. The plant interconnecting transformer also has a delta-wye-grounded connection and has a leakage reactance of 0.1 pu on the 300 MVA base.

Each inverter is rated at 480 V and operates with a switching frequency of 9 kHz. The dc link voltage is maintained at 1.5 kV. Fig. 2 shows the simplified control scheme. A closed-loop controller (not shown in Fig. 2) adjusts the positive-sequence reference to obtain the desired active power and power factor.

When a voltage dip occurs at the IBR terminals, the fault-detection logic (not shown in Fig. 2) freezes both the positive-sequence reference and the PLL at values recorded one-quarter cycle before the disturbance. As a result, the inverter current controller in Fig. 2 receives the frozen (pre-fault) positive-sequence current reference along with the live (fault) reactor currents.

For bolted faults at the inverter terminals, we select the virtual reactor impedance to ensure that the IBR current remains within the capability of the inverter semiconductor devices. We choose the X/R ratio to obtain the desired angle of the negative-sequence impedance. In this study, we selected the impedance of the virtual shunt reactor as 0.045 + j0.3016 Ω for an individual 1 MVA, 480 V unit.

The inverter current controller tracks the dc components of the d and q currents, which represent the positive-sequence component, and their double frequency components, which represent the negative-sequence component of the reactor currents. The bandwidth required to generate the IBR currents is well within the inverter capabilities when operating at the 9 kHz switching frequency (see Subsection VII.F for an illustration).

B. Relay Playback

We tested the response of relays [1] and [6] to fault conditions in the system shown in Fig. 5. Both relays responded as expected.

In this section, we use relay [1] to illustrate the impact of the proposed IBR fault response method on line protection. The

relay allows direct digital playback by uploading IEEE COMTRADE files into its memory and executing the playback command. This capability allows us to test practical relay subsystems, including frequency tracking, phasor estimation, voltage-polarizing (memory) logic, and incremental quantity derivation and filtering. In the following subsections, we use secondary quantities based on a 2,000:1 voltage ratio and a 1,600:5 current ratio.

The relay [1] uses a variable-window phasor estimator. At the fault inception, the relay resizes the window to a fraction of a cycle. The window then expands as it slides until it reaches a full cycle. These phasors typically settle within about a half cycle while preserving the accuracy of full-cycle estimators during fault steady-state conditions.

We used a 50 ms window (3 cycles in a 60 Hz system) for plotting the incremental positive-sequence voltage and current. Consequently, these incremental signals are valid only during the first 3 cycles of a fault. After 50 ms, we force these signals to zero to avoid confusion.

The relay includes an instantaneous directional element based on incremental quantities (TD32). This element applies low-pass filtering for security and uses a one-cycle memory when deriving incremental quantities.

Appendix G of [1] provides a detailed description of signal processing for all major relay subsystems. This description is sufficient to fully reproduce our results.

Because our approach freezes the PLL (or alternatively applies a deliberately long time constant in the PLL controller once the PLL has locked to the live voltage), we do not expect significant changes in the measured frequency or the voltage-polarizing logic during the first few cycles of a fault. Our tests confirmed that the frequency measurement remains very stable and the polarizing logic provides proper polarization for the mho distance elements.

C. Symmetrical Three-Phase Fault

We begin with a symmetrical three-phase fault to demonstrate the response of the positive-sequence and incremental quantities. During symmetrical faults, both the zero- and negative-sequence components equal zero, allowing us to focus on the positive-sequence and incremental quantities. Fig. 6 shows currents, voltages, and selected derived signals for a remote-end three-phase line fault (all examples in this section use remote-end faults, i.e., faults located at a distance of 50 km).

The instantaneous IBR fault current peaks at 1.56 pu and settles at 1.12 pu during the fault.

The positive-sequence impedance ΔZ_1 (see (1)), which connects the incremental positive-sequence voltage and current, stabilizes at approximately 45 Ω secondary and 85 degrees. The impedance stabilizes in about 10 ms (just over a half cycle). This short settling time reflects the variable-window phasor estimation in the relay, but it also demonstrates the effectiveness of the proposed time-domain control method in regulating the IBR fault current.

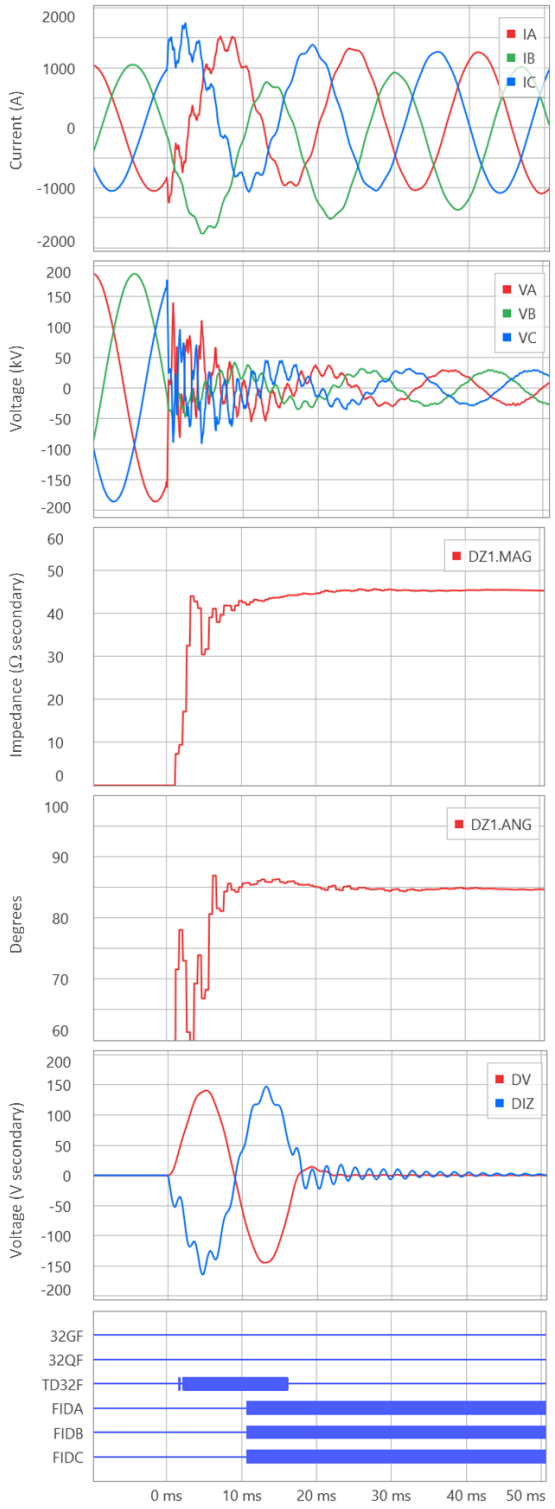


Fig. 6. Remote-end symmetrical three-phase fault example.

The impedance plot is very stable, indicating accurate reproduction of the virtual shunt reactor currents without interference from the positive-sequence current controller. Because the incremental positive-sequence voltage and current are tied through a fixed inductive impedance (see Fig. 4c), a directional protection element based on these incremental quantities provides reliable directional discrimination for this symmetrical fault and any other fault type.

Fig. 6 also illustrates the response of the time-domain incremental loop voltages and currents by using the BC loop as an example. Fig. 6 shows the incremental voltage (Δv_{BC}) and incremental replica current (Δi_{ZBC}) scaled – for ease of comparison – by using the expected reactor impedance of 45 Ω secondary. Also, the relay applies a low-pass filter to reject high-frequency components present in the terminal voltages and currents. For a forward fault, the two signals should track each other with opposite polarities. Fig. 6 shows a near-perfect polarity relationship. An incremental-quantity directional element, such as the TD32 element in [1], provides reliable directional protection for this symmetrical fault and any other fault type.

The relay correctly identified the fault type (FIDA, FIDB, and FIDC asserted) and, by using a single-ended impedance-based method, calculated the distance to the fault as 50.048 km.

D. Phase-to-Phase Fault

We use an unbalanced fault that does not involve ground to demonstrate the weak system characteristic of IBR installations and to avoid the assistance of zero-sequence current present during ground faults. This example highlights the stability of the negative-sequence fault response and its consistency with the incremental positive-sequence response. Fig. 7 shows the currents, voltages, and selected derived signals for a remote-end resistive BC line fault with a fault resistance of 5 Ω primary. The instantaneous IBR fault current peaks at 1.62 pu and settles at 1.27 pu during fault conditions.

The incremental positive-sequence impedance (ΔZ_1) stabilizes near 45 Ω secondary and 84 degrees, while the negative-sequence impedance (Z_2) settles at approximately 46 Ω secondary and 88 degrees. Ideally, these two impedances should match because the same virtual shunt reactor, without mutual coupling, produces both the negative-sequence current and the incremental positive-sequence current (see Fig. 4c). We attribute these minor differences between the ΔZ_1 and Z_2 values to the accuracy limits of the inverter current controller (see Fig. 1). Both impedances are stable and inductive, enabling robust directional protection, and their minor differences in magnitude and angle are inconsequential. Importantly, the negative-sequence impedance stabilizes almost immediately (in about three-quarters of a cycle), with the duration of its transient determined only by the phasor estimator window length. There is no delay between fault inception and the appearance of a stable negative-sequence current.

Fig. 7 shows the angle between the incremental positive-sequence current and the negative-sequence current. As expected for a BC fault, this angle is close to 180 degrees (177 degrees). Fig. 7 also shows the single-ended impedance-based fault location result by using the negative-sequence current as a polarizing signal, properly shifted to compensate for the network nonhomogeneity. The fault location estimation settles at 49.8 km. This result demonstrates that a distance relay polarized with the negative-sequence current also functions correctly.

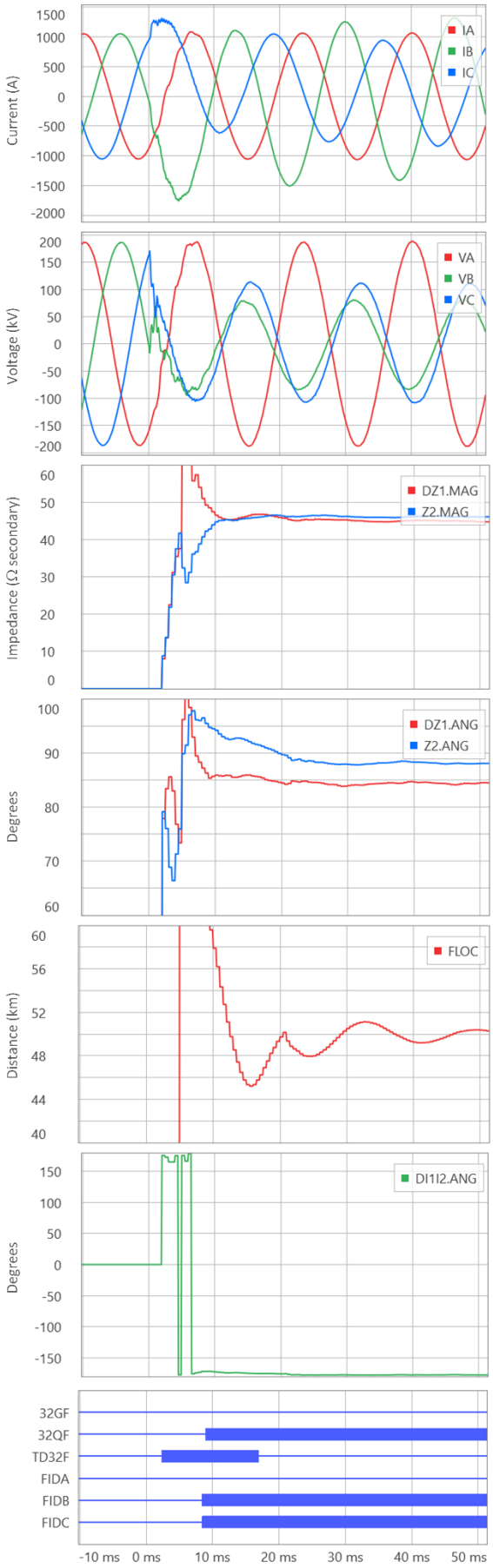


Fig. 7. Remote-end phase-to-phase fault example.

The relay responded correctly in terms of the incremental-quantity directional protection element (TD32), the negative-sequence directional protection element (32Q), and the faulted-loop selection logic (FIDB and FIDC asserted).

E. Evolving Fault

Evolving faults pose a significant challenge for any IBR fault response standard. At the instant a fault evolves, for example, from an initial AG fault to an ABG fault, the negative-sequence voltage changes. The negative-sequence current in any IBR fault response standard must track both the magnitude and angle of this voltage. If the standard allows a generous margin for current adjustment, such as 50 ms, as prescribed in [5], the current may lag and never align with the evolving voltage. Initially, the current attempts to follow the original voltage angle, but before it settles, the voltage shifts again as the fault evolves. By the time the current begins tracking the new voltage, the fault may already be cleared. In such cases, the IBR remains compliant with [5], yet the negative-sequence current is never fully coherent with the negative-sequence voltage.

Fig. 8 illustrates currents, voltages, and selected derived signals for a remote-end AG line fault that evolves into an ABG fault within 96 ms. The instantaneous IBR fault current peaks at 1.46 pu and settles at 1.21 pu during the fault. Although Fig. 8 shows currents higher than 1.46 pu, the line currents are elevated by the zero-sequence component contributed by the interconnecting transformer, and the IBR currents remain relatively small.

The incremental positive-sequence impedance (ΔZ_1) stabilizes near 44.9 Ω secondary and 84 degrees, while the negative-sequence impedance (Z_2) settles at approximately 45 Ω secondary and 87 degrees. When the fault evolves at 96 ms, the negative-sequence voltage changes, as does the current, yet the apparent impedance remains relatively stable. This steady impedance response demonstrates the accuracy of our method in emulating the desired fault behavior in the time domain.

Fig. 8 also shows the angle between the negative- and zero-sequence currents. In a perfectly homogeneous network, this angle should be 0 degrees during an AG fault and 120 degrees during an ABG fault. In our example, the angles are –6 degrees and 113 degrees, respectively. This close match confirms that a traditional faulted-loop selection logic would operate correctly in our approach. Typically, the logic uses a 30-degree threshold, so deviations of 6 degrees and 7 degrees are well within acceptable margins.

We can explain the coherence between the negative- and zero-sequence currents as follows: the zero-sequence current aligns with the zero-sequence voltage based on the interconnecting transformer impedance, while the negative-sequence current aligns with the negative-sequence voltage based on the virtual shunt reactor impedance. Because the zero- and negative-sequence voltages are coherent (both result from the same fault), and their corresponding currents are also coherent. Any angle differences between these currents arise from the impedance angle differences behind the relay.

This negative- and zero-sequence current angle alignment confirms that the network remains homogeneous in our approach. The incremental phase currents, incremental positive-sequence current, negative-sequence current, and zero-sequence current all have the same angle (the impact of the fault type notwithstanding). This common angle matches the angle of the current flowing in the fault path, ensuring proper polarization of reactance comparators in quadrilateral distance protection elements and impedance-based fault locators. Fig. 8 shows that the fault location value stabilizes at about 49.9 km.

F. IBR Control Illustration

We also use the evolving fault example to illustrate the IBR control action. Fig. 9 shows the per-unit phase-to-phase voltages at the IBR terminals. Our method uses these voltages to calculate the virtual reactor currents as described in Section IV. The reactor currents decrease from the pre-fault value of 0.768 pu following the AG fault and change again when the fault evolves into an ABG fault at 96 ms. As expected for currents in an inductive circuit, the virtual reactor currents exhibit decaying dc offsets and no abrupt changes. The reactor currents follow the IBR voltages in terms of transient behavior, including decaying dc offsets and high-frequency oscillations, and in terms of voltage phasor changes due to the fault evolution. This delay-free relationship between the measured voltages and the virtual reactor currents is central to the proposed method.

With reference to Fig. 2, the controller transforms the virtual reactor currents from the ABC reference frame into the dq frame and then sums them with the positive-sequence currents, also expressed in the dq frame. The positive-sequence reference currents are frozen at their pre-fault values as soon as the fault-detection logic asserts. The resulting dq-frame IBR currents are passed to the inverter current controller shown in Fig. 2, resulting in the IBR terminal currents shown at the bottom of Fig. 9. Effectively, the IBR maps the voltages into currents, assuming frozen pre-fault positive-sequence current and the presence of a virtual reactor at the IBR terminals.

Of course, the IBR currents in Fig. 9 are in per unit and are measured on the low-voltage side of the transformer, whereas the relay currents in Fig. 8 are in primary amperes and measured on the high-voltage side of the transformer.

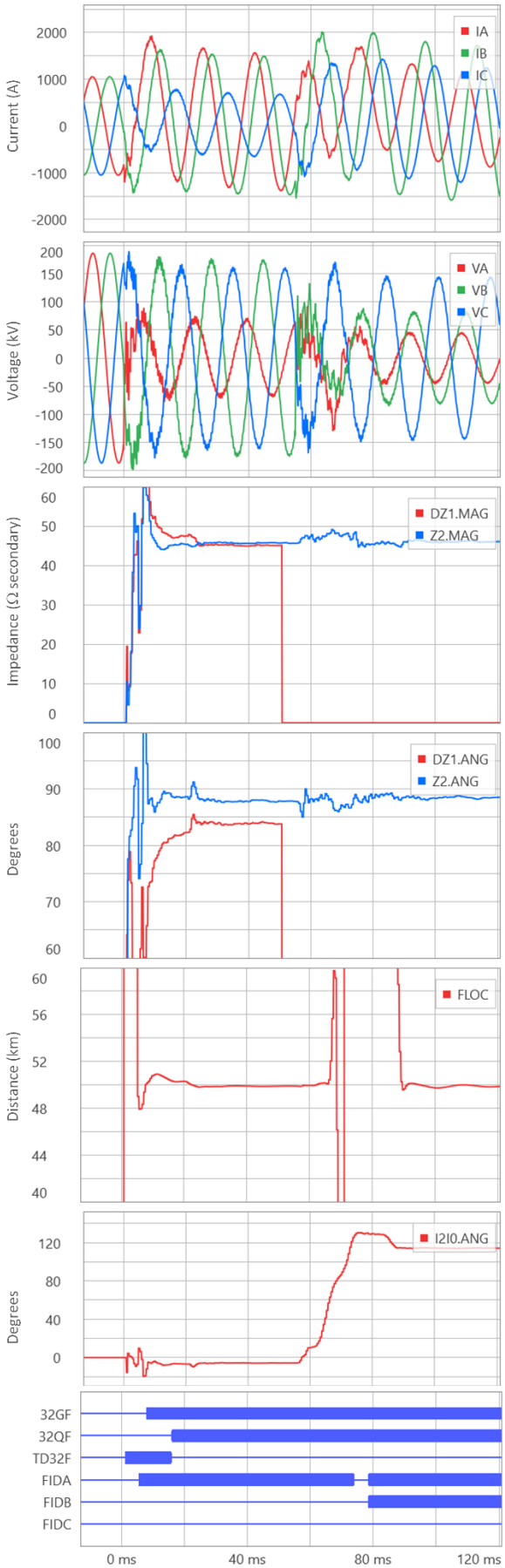


Fig. 8. Remote-end evolving fault example (AG → ABG).

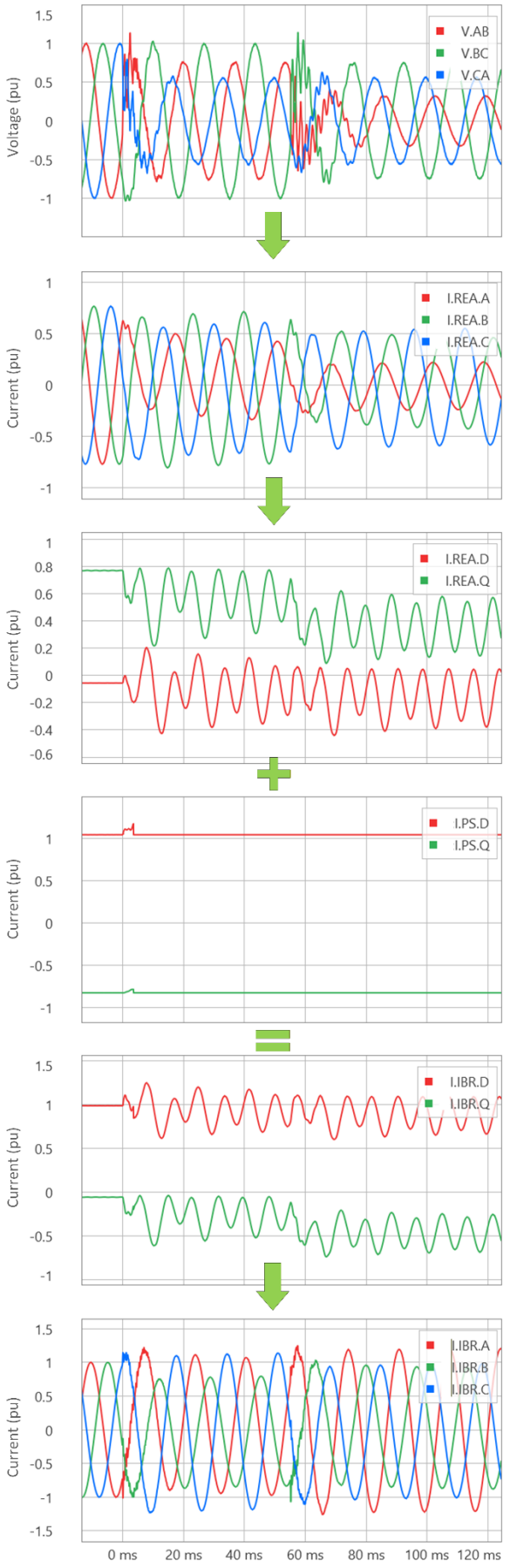


Fig. 9. IBR per-unit signal flow for the case in Fig. 8.

VIII. IBR Standards Harmonization

The present IBR fault-response standards can incorporate the proposed approach as follows:

- Introduce a requirement to defer control actions until several cycles into the fault. These actions include reactive power injection, synthetic inertia, and similar functions.
- Mandate that the negative-sequence current appears without a time delay, which requires a time-domain implementation.
- Specify that the incremental positive-sequence impedance matches the negative-sequence impedance, thereby endorsing the virtual shunt reactor concept.
- Require that the positive-sequence current controller and the PLL remain unchanged during the initial few cycles of a fault.

These recommendations represent either new requirements or adjustments to the parameters of existing ones, and therefore, they can be incorporated without undoing prior standardization work.

IX. Conclusions

In this paper, we proposed reframing the discussion on IBR response during fault conditions. We recommend the following:

- Focus on incremental currents, including the negative-sequence current, to achieve the desired fault current characteristics without compromises, rather than focusing on total currents and accepting compromises.
- Prioritize fault current asymmetry (pattern) and coherence with the voltages, rather than prioritizing fault current magnitude and angle.
- Prioritize fast fault response, rather than allowing a generous margin for the desired fault current response time and leaving protective relays with uncontrolled current characteristics at the beginning of the fault.
- Specify and implement the fault response in the time domain, rather than by using phasors while allowing generous settling times.
- Prevent auxiliary functions, such as low-voltage ride-through, from engaging too early. Instead, prioritize creating favorable conditions for protection operation within the first few cycles while not allowing these functions to activate and create additional challenges for the relays.

The paper explains how to implement the proposed IBR fault current response logic and illustrates its performance with examples. We used a generic IBR model with standard controllers and an inverter. We did not modify or optimize these models, yet the results were highly encouraging.

The proposed method is simple: freeze the positive-sequence current controller, including the PLL, for the first few cycles of a fault (or longer) and emulate a virtual shunt reactor. The virtual reactor logic is engaged permanently, further simplifying implementation by avoiding switching it on and off. The simplicity should encourage IBR manufacturers to adopt, refine, and implement this method.

Our method eliminates the need to model IBR fault response for setting instantaneous protective relays in high-voltage networks. The IBR behaves as a current source with unchanged load current and superimposed incremental currents, including the negative-sequence current, that remain coherent with the voltages. Short-circuit analysis programs should represent IBRs that follow our method by using the equivalent network shown in Fig. 4c.

Our approach offers the following benefits for high-voltage protection systems:

- Directional protection becomes available for all fault types, including negative-sequence directional elements and incremental directional elements.
- Faulted-loop selection remains possible by using the traditional principle of comparing the negative- and zero-sequence current angles.
- The network remains homogeneous, maintaining expected angle relationships among incremental currents, including the negative-sequence current, and between these currents and voltages. This homogeneity supports advanced protection methods beyond directionality and faulted-loop selection, including reactance polarizing in distance protection elements and impedance-based fault locating.
- Distance protection elements perform reasonably well. Mho distance elements benefit from the “frozen” PLL that remains at the pre-fault angle and frequency, which ensures accurate memory polarizing voltage. Quadrilateral distance elements benefit from the preserved network homogeneity, enabling current-based polarization of reactance comparators.
- Line current differential schemes also benefit from network homogeneity. The differential current effectively acts as an incremental signal: it represents the fault current components by excluding the load current component. The preserved network homogeneity ensures that, for internal faults, the local and remote fault current components are almost in phase, maximizing the differential current and allowing the differential scheme to operate more reliably.

Being simple yet providing traditionally expected fault signal characteristics, our approach has the potential for widespread adoption by users, IBR manufacturers, and standardization bodies. It also allows relay manufacturers to leverage existing protection implementations based on incremental quantities, as well as develop new protection elements and schemes that take advantage of how IBRs behave when following our approach.

X. Acknowledgment

The authors would like to thank Mr. Mangapathirao V. Mynam of Schweitzer Engineering Laboratories, Inc., for conducting the laboratory tests and for providing other valuable contributions to this work.

XI. References

[1] *SEL-T401L Instruction Manual*. Available: selinc.com.

[2] E. O. Schweitzer, B. Kasztenny, M. V. Mynam, N. Fischer, and A. Guzman, "Solving Line Protection Challenges With Transient-Based Relays," *Protection, Automation, Control World Magazine*, No. 63, March 2023, pp. 28–33. Available: https://www.pacw.org/issue-063-march-2023.

[3] B. Kasztenny, "Line Distance Protection Near Unconventional Energy Sources," *16th International Conference on Developments in Power System Protection*, Newcastle, UK, 2022, pp. 224–229, 10.1049/icp.2022.0944.

[4] CIGRE TB 575 Benchmark Systems for Network Integration of Renewable and Distributed Energy Resources, 2014.

[5] IEEE Std. 2800-2022, *IEEE Standard for Interconnection and Interoperability of Inverter-Based Resources (IBRs) Interconnecting With Associated Transmission Electric Power Systems*, April 2022, 10.1109/IEEESTD.2022.9762253.

[6] *SEL-411L Instruction Manual*. Available: selinc.com.

XII. Biographies

Bogdan Kasztenny has 35 years of experience in power system protection and control. In his decade-long academic career (1989–1999), Dr. Kasztenny taught power system and digital signal processing courses at several universities and conducted applied research for several relay manufacturers. In 1999, Bogdan left academia for relay manufacturers where he has since designed, applied, and supported protection, control, and fault-locating products with their global installations numbering in the thousands. Bogdan is an IEEE Fellow, an IET Fellow, a Senior Fulbright Fellow, a Distinguished CIGRE Member, and a registered professional engineer in the province of Ontario. Bogdan has served as a Canadian representative of the CIGRE Study Committee B5 (2013–2020) and on the Western Protective Relay Conference Program Committee (2011–2020). In 2019, Bogdan received the IEEE Canada P. D. Ziogas Electric Power Award. Bogdan earned both the PhD (1992) and DSc (Dr. habil., 2019) degrees, has authored over 250 technical papers, and holds over 60 U.S. patents.

Normann Fischer received a Higher Diploma in Technology with honors from Technikon Witwatersrand, Johannesburg, South Africa, in 1988; a BSEE with honors from the University of Cape Town in 1993; an MSEE from the University of Idaho in 2005; and a PhD from the University of Idaho in 2014. He joined Eskom as a protection technician in 1984 and was a senior design engineer in the Eskom protection design department for three years. In 1999, Normann joined Schweitzer Engineering Laboratories, Inc. (SEL), where he is currently a vice president and distinguished engineer in the Research and Development division. He has authored and coauthored more than 80 technical papers and 12 transactions papers. He holds more than 30 patents related to electrical engineering and power system protection. He is currently an IEEE Fellow and a member of the American Society for Engineering Education (ASEE).

Ali Hooshyar is a Canada Research Chair in electric power systems and an Associate Professor with the Department of Electrical and Computer Engineering, University of Toronto, Toronto, ON, Canada. His research interests include dynamics, control, and protection of renewable energy systems. Dr. Hooshyar is an Editor of IEEE Transactions on Smart Grid, IEEE Transactions on Power Delivery, and IEEE Power Engineering Letters. He was the Guest Editor-in-Chief of the Special Issue of IEEE Transactions on Power Delivery on "Resilience-Oriented Protection, Control, and Monitoring Systems for Power Grids." Dr. Hooshyar was the Guest Editor of the IEEE Electrification Magazine for the Special Issue on "Microgrid Protection and Control." He is also an Associate Editor for the Wiley Encyclopedia of Electrical and Electronics Engineering. Dr. Hooshyar is a senior member of the IEEE and chairs Working Group C45 of the IEEE Power Systems Relaying and Control Committee on short-circuit modeling and protection of power systems with high penetration of inverter-based resources.

© 2026 by Schweitzer Engineering Laboratories, Inc. and
University of Toronto
All rights reserved.
20260225 • TP7255-01